Journal of Science and Technology − Smart Systems and Devices
Volume 36, Issue 3, September 2026, 060–066

Fundamental Experiments on Stopping Control of a Scaled Model Propeller Aircraft Using Double-Fan Propulsion System

Tetsu Miyazaki, Hideki Toda*
Faculty of Engineering, University of Toyama, Toyama, Japan
**Corresponding author email: toda@eng.u-toyama.ac.jp*

Abstract

The motion of ships and aircraft is governed by inertia and hydrodynamic or aerodynamic forces, so they do not stop immediately even when reverse thrust is applied. Consequently, operations such as maneuvering in harbors and landing require control that can decelerate and stop accurately near a target position, yet full-scale testing can be costly and constrained by safety. This study uses a small wheeled model equipped with two coaxial propellers forming an independently actuated double- fan propulsion system and examines stopping control experimentally. Position is estimated from an overhead camera by detecting a red marker on the vehicle and computing its centroid. Manual control, proportional position control, fixed- reverse thrust commands, and reference-velocity-based control using velocity feedback were compared. In Experiment 1, fixed- reverse command levels were varied to characterize stopping behavior. In Experiment 2, a single operator controlled the forward thruster while position-based reverse thrust was applied automatically. In Experiment 3, a reference velocity profile obtained from successful manual runs was used for velocity-based control. The results show that fixed reverse thrust can change stopping accuracy and trajectory dispersion depending on the command level, while the reference-velocity-based controller reduced the average stopping-position overshoot from approximately 9 mm to 3 mm under the tested conditions. The contribution of this study is not a new derivative-control law, but an experimental characterization of independently actuated forward/reverse fan control and the application of a reference-velocity-based stopping strategy to this specific double-fan platform. The results are limited to the tested small-scale model and are not intended as a quantitative prediction of full-scale aircraft behavior.

Keywords: Double-fan propulsion, reference velocity, reverse thrust, stopping control, velocity feedback.

1. Introduction

Vehicles such as propeller-driven aircraft and ships include inertial terms in their equations of motion and are subject to fluid forces (drag, lift, induced flow around propulsors, etc.) [1, 2]. Therefore, even when re-verse thrust (reverse operation) is commanded, they do not stop immediately and tend to overshoot the target position.

Fig. 1(a) illustrates a thrust-reverser mechanism on an aircraft engine. During forward thrust the doors are closed; during reverse thrust they open and turn the for-ward airflow to exhaust forward, producing a decelerating effect. Without such devices, aircraft could not land safely and stop within short distances with high accuracy, yet operation and control remain largely manual and automation is challenging [3-7]. Similarly, berthing maneuvers in harbors require skilled manual control (Fig. 1(b)) [8-12].

In scenarios such as harbor berthing and aircraft landing, where deceleration and stopping must be achieved safely within limited distance, the accuracy and repeatability of stopping control are critical [13-16].

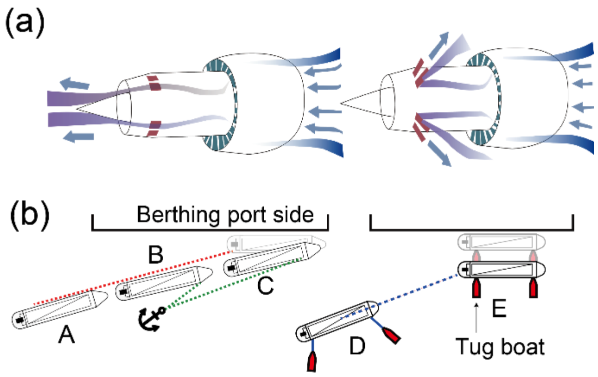

Fig. 1. Examples of reverse thrust in aircraft and berthing operations in ships

The cited literature includes ship-control studies on berthing, low-speed maneuvering, and automatic positioning [1, 3-19], aircraft motionand control [2], and multi-fan or counter-rotating fan systems such as the ducted counter-rotating axial-flow fan system reported in [25]. However, the present study focuses specifically on stopping-position control of a small wheeled platform with independently commanded forward and reverse

p-ISSN 3093-3285
e-ISSN 3093-3315
https://doi.org/10.51316/jst.192.ssad.2026.36.3.7
Received: Jul 16, 2026; Revised: Aug 21, 2026;
Accepted: Sep 8, 2026; Online: Sep 14, 2026

fans. In this configuration, two actuators act along the same translational axis, creating a redundant input structure: if f_f and f_r denote the forward and reverse thrust magnitudes, the idealized net longitudinal force can be represented as $f_{\text{net}} = f_f - f_r$. Different actuator-command combinations can therefore produce similar net force, while motor dynamics and airflow interaction can further complicate the input-output relationship. The present work addresses this experimental gap by investigating stopping control with the independently actuated double-fan propulsion system. The study has three specific contributions: (1) experimental characterization of stopping behavior when the forward and reverse propulsion paths are operated independently; (2) evaluation of fixed reverse-thruster commands and their effect on stopping accuracy and trajectory dispersion; and (3) experimental evaluation of a reference-velocity-based controller derived from successful manual stopping trajectories. The derivative/velocity-feedback principle itself is conventional; the contribution is its application and experimental evaluation for the present double-fan stopping problem. Because the platform is a small-scale, ground-constrained model, the results are interpreted as experimental findings for the tested system rather than as direct scaling laws for a full-scale aircraft.

2. System Under Study

2.1. Vehicle Overview

We consider a scaled propeller aircraft (180 mm × 150 mm × 50 mm) and restrict attention to straight-line motion along the x-axis on a flat floor. The vehicle mass is 85 g. The propulsion system is a double-fan arrangement with two coaxial propellers—forward and reverse—so that forward thrust and reverse thrust can be commanded independently (Fig. 2). The model is used as a ground-constrained experimental platform; it is not operated as a free-flying aircraft in the present study. Consequently, pitch attitude, angle of attack, and longitudinal flight stability are outside the scope of the experiments.

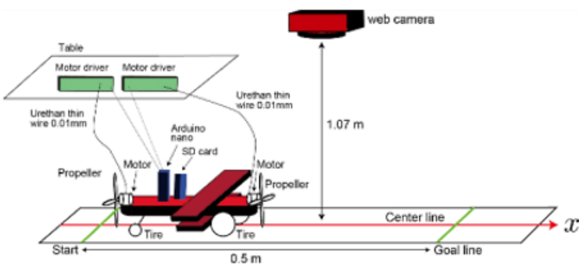

Fig. 2. System under study: scaled model propeller air-craft and schematic of the double-fan propulsion system

2.2. Position Estimation

Vehicle position is estimated from overhead camera imagery (Fig. 3). A red marker on the vehicle is detected and its centroid yields the position in image coordinates. Given the camera resolution, the position estimate was accurate to approximately 1 mm.

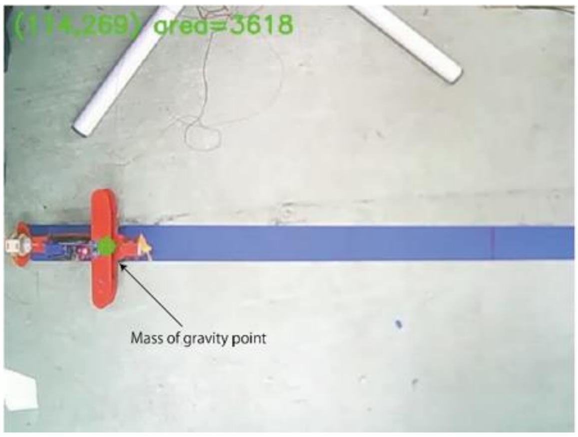

Fig. 3. Overview of position estimation (red-marker detection and centroid computation)

3. Control Architecture

Actuation uses a dual-FET motor driver (separate channels for forward and reverse) and a microcontroller based on an Arduino Nano. The Arduino Nano is mounted on top of the airframe; measurements are logged to an SD card. The two-channel motor driver is placed on the desk because of its mass; PWM commands from the microcontroller to the driver, and driver outputs to the motors, are carried through light 0.01 mm urethane wires so as not to disturb vehicle motion.

3.1. Manual Control

In manual mode, a 10kΩ joystick-style potentiometer is adjusted by hand; its angle is read by the microcontroller ADC and mapped to thrust commands (Fig. 4). Throughout this study, manual operation serves as the baseline for comparison with feedback strategies.

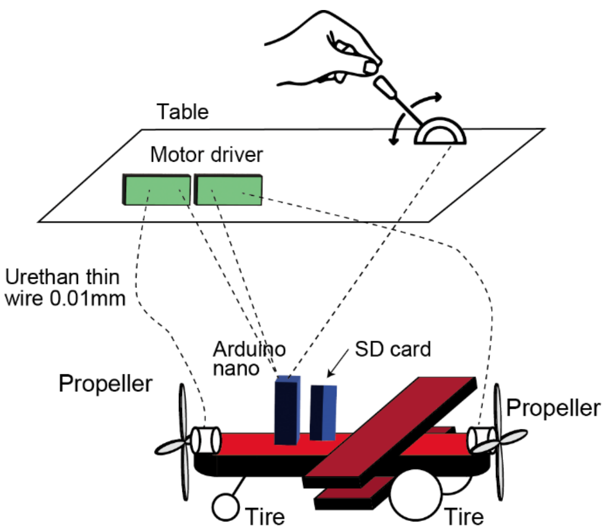

Fig. 4. Manual control (thrust command from the potentiometer)

3.2. Challenges of Position Control with Fan Actuators

The plant studied here faces several difficulties inherent to fan-based actuation. First, thrust cannot be measured directly; the reaction force produced through the air from motor voltage must be used indirectly as thrust. Second, fan dynamics involve intrinsic delay and a continuously changing medium, making it hard to identify that delay a priori for controller design. Third, the air state aroundthefan is not directlyobservable, and turbulence generated by the fan increases thrust uncertainty [20, 21]. With two opposing actuators acting along the same translational axis, the net longitudinal force depends on the combined effect of the two actuator commands. In an idealized form, $f_{\text{net}} = f_{\text{f}} - f_r$, so different forward/reverse command pairs can produce similar net force. This redundant input structure can make command allocation and controller tuning more difficult, while airflow interaction between the two fans can further complicate the actual input-output relationship [22-25].

4. Experiments

4.1. Experimental Setup

Fig. 5 shows the test environment. A straight track marked in blue was prepared for motion along one axis, with an overhead camera for position estimation. The vehicle length is approximately 180 mm and mass 85 g. The track length is 1000 mm; the distance from the initial position to the target is 500 mm. The floor is flat with negligible friction.

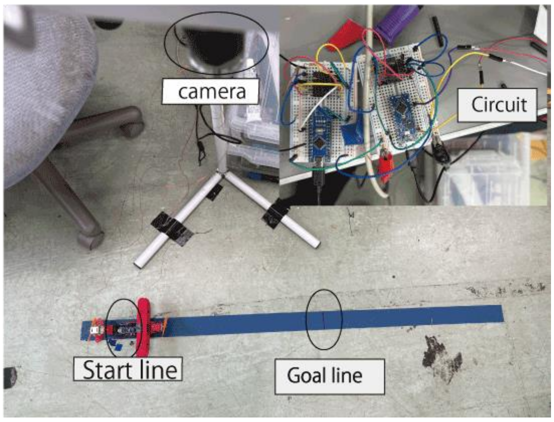

Fig. 5. Experimental environment

4.2. Experiment 1: Stopping Behavior under Fixed Reverse Thrust

In Experiment 1 we compare stopping position and dispersion after a stop command under (a) forward or reverse thruster used alone, and (b) forward thruster with the reverse thruster additionally engaged.

Case (a) evaluates forward motion and stopping when only the forward thruster or only the reverse thruster is active. Note that the stern reverse thruster produces forward-pointing thrust by spinning the propeller in the opposite direction relative to normal forward operation, which degrades thrust performance relative to the design direction of rotation. Control follows the laws below.

$$f_{\text{forward}} = K_{pf}(x_0 - x) \quad (1)$$

$$f_{\text{reverse}} = -K_{pr}(x_0 - x) \quad (2)$$

Here f_{forward} and f_{reverse} are PWM commands to the forward and reverse thrusters, K_{pf} and K_{pr} are their proportional gains, x_0 is the target position, and x is the current position. The PWM command values are dimensionless controller inputs on a 0–255 scale and are not direct measurements of thrust force. Simple proportional control was adopted to examine basic properties of fan-based position tracking [25].

Under condition (b), the forward thruster follows proportional control while the reverse thruster applies a fixed PWM command f_r . With (2) alone, the reverse-thrust command cannot provide the required braking action before the target while the vehicle is still on the approach side; therefore, a constant reverse command was tested to provide braking before the target and to assess how the independently actuated reverse path affects stopping behavior.

$$f_{\text{forward}} = K_{pf}(x_0 - x) \quad (3)$$

$$f_{\text{reverse}} = f_r \quad (4)$$

Several levels of fixed reverse-thrust command were tested over a broader range. Here, f denotes the PWM command value applied to the reverse thruster (0–255). The representative values f_r = 75, 125, 250, max 255 = 6.5 V) were used to study trends in stopping behavior (Fig. 7).

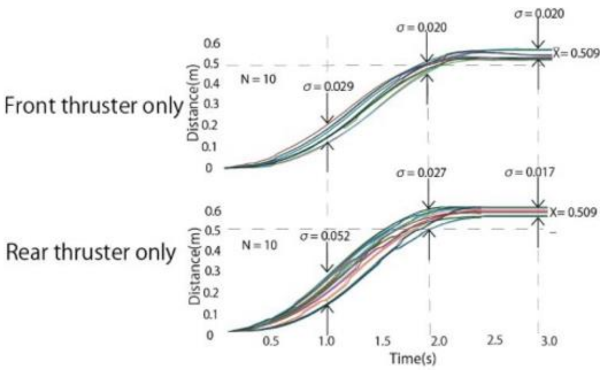

Fig. 6. Results for Experiment 1(a). Top: approach control using only the forward thruster. Bottom: approach control using only the reverse thruster

Fig. 7 shows Experiment 1(b) for three reverse levels. Final-position accuracy tended to improve over Experiment 1(a). Notably, accuracy was better for low (f_r = 75) and high (f_r = 250) reverse commands, whereas intermediate reverse (f_r = 125) worsened accuracy. Trajectory bulging near x ≈ 1.0 m was also worst at f_r = 125 and smaller for the other two conditions.

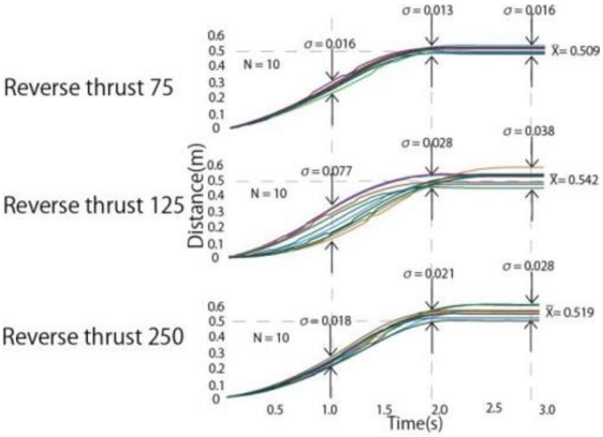

Fig. 7. Results for Experiment 1(b): proportional control on the forward thruster and fixed PWM command on the reverse thruster. Representative reverse-thruster commands are f_r = 75, 125, and 250: the maximum PWM command is 255

Fig. 8(a) summarizes Experiment 1(b): the curves show the temporal standard deviation for each f_r condition. The standard deviation peaks near t = 1.0 s at the mid-track for f_r = 125. Fig. 8(b) reports a finer sweep of fr to check whether the effect is unique to 125. A sharp peak at f_r = 125 suggests nonlinear, hardware-specific behavior.

4.3. Experiment 2: Manual Forward Control with Position-Based Proportional Reverse Thrust

Experiment 2 evaluates a single-operator forward-control condition combined with position-based proportional reverse thrust. Its purpose was to examine whether an automatically imposed position-based braking input produces stopping behavior consistent with the manual forward-thrust strategy observed in Experiment 1. This experiment was not designed as a multi-participant human-factors study.

$$f_{\text{forward}} = \text{human control} \tag{5}$$

$$f_{\text{reverse}} = -K_{pr}(x_0 - x) \tag{6}$$

A single operator (the first author) continuously commanded the forward thruster while reverse thrust from (6) was superimposed, and dispersion in the stopping position and overshoot were assessed (Fig. 9). More than 100 practice runs were conducted. Because only one operator participated, demographic comparisons, inter-subject variability, and standardized between-subject instructions were not part of the experimental design. As the sole participant was one of the authors, no separate written informed consent was required; the author voluntarily performed the trials with full knowledge of the experimental procedure, which involved operating a low-power (≤6.5 V) desktop-scale model and posed no more than negligible physical risk.

The trajectories nevertheless exhibited large bulging and variation in the final positions.

(a)

Reverse-thrust	σ (1.0)【m】	σ (1.8)【m】	σ (2.8)【m】	Average stop position 【m】
75	0.016	0.013	0.016	0.509
125	0.077	0.028	0.038	0.542
250	0.018	0.021	0.028	0.519

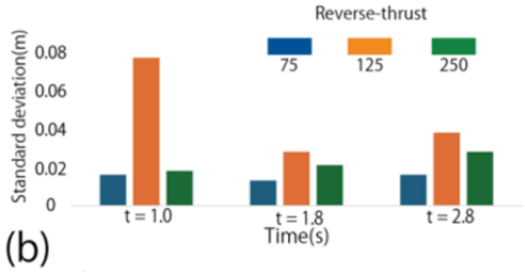

(b)

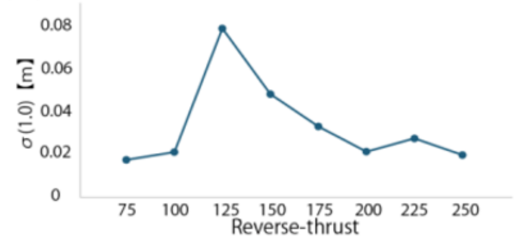

Fig. 8. (a) Summary of Experiment 1(b). (b) Follow-up experiment varying the fixed reverse-thrust level to reassess dispersion in the final position

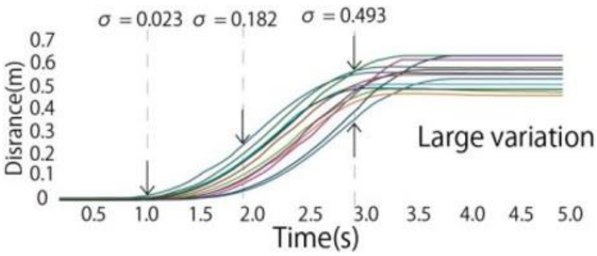

Fig. 9. Results for Experiment 2 (manual forward thrust + proportional reverse thrust)

4.4. Experiment 3: D Control with a Reference Velocity Profile from Successful Manual Runs

Motivated by the single-operator results in Experiment 2, we tested the hypothesis that stopping performance can be improved when the controller uses velocity information in addition to position error. Repeated successful manual runs were used to build a reference trajectory, and its time derivative yielded a desired speed profile. We then designed reference-velocity-based control using velocity feedback. This approach should not be interpreted as a new derivative-control principle; rather, it was used to test whether experimentally derived speed information could improve stopping performance in the double-fan configuration.

$$f_{\text{forward}} = f_0 + K_d\big(v - V_0(t)\big) \tag{7}$$

$$f_{\text{reverse}} = f_0 - K_d\big(v + V_0(t)\big) \quad (8)$$

Here f_0 is a thrust bias, $V_0(t)$ the reference speed, and v the measured speed. Reference speeds were assigned at 0.1 m waypoints along the path.

The control sequence was: (1) From the start to 0.1 m, command maximum thrust $f = 250$ and hold a peak reference speed of 0.3 m/s. (2) From 0.2 m before the target, apply reverse (braking) according to (8) while the forward thrust follows (7), decaying both commands to suppress inertial overshoot and reduce speed to 0.05 m/s at the end.

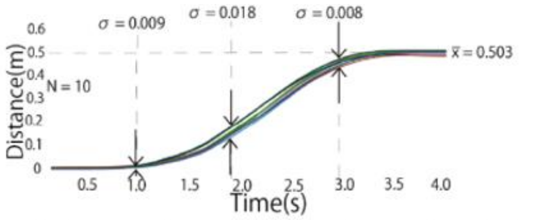

	σ(1.0)	σ(1.8)	σ(2.8)	X̄
Exp.3	0.009	0.018	0.008	0.503
Exp.1	0.016	0.013	0.016	0.509

Fig. 10. Results for experiment 3

Before Experiment 3, the control parameters in (8) were tuned heuristically to realize the desired speed profile and accurate stopping. Fig. 10 shows Experiment 3 for N = 10 repeated trials; trajectory spread and final-position variability are reduced, yielding stable behavior. The lower panel compares against forward-thruster-only control from Experiment 1; except for bulging near t ≈ 1.8 s, Experiment 3 is superior across the metrics shown.

4.5. Discussion

4.5.1. P Control exhibited oscillatory behavior

The proportional controller generated thrust solely from the position error. As the vehicle approached the target position, a considerable amount of kinetic energy remained because of inertia. Consequently, the controller could not anticipate future motion and reacted only after the position error changed. This behavior resulted in repeated acceleration and deceleration around the target position, producing the overshoot and oscillatory trajectories observed in Fig.6.

In addition, the fan propulsion system contains delays associated with motor dynamics and airflow generation. Because thrust is not produced instantaneously, the actual vehicle response lags behind the control input. Such delays are considered to have further amplified the oscillatory behavior; however, a detailed analysis of the propulsion dynamics is beyond the scope of the present study.

Comparing Experiment 1(a) and 1(b) also provides indirect evidence for the advantage of independently actuated forward/reverse fans over a single-actuator scheme such as throttle reduction or a single reversible propeller. In Experiment 1(a), each actuator operated alone, analogous to relying solely on drag-based deceleration (throttle reduction) or a single bidirectional thruster. In Experiment 1(b), applying both actuators independently and simultaneously improved final-position accuracy over either single-actuator condition (Fig. 6 vs. Fig. 7). This suggests that decoupling the forward and reverse thrust paths — rather than relying on a single actuator to both propel and brake — is itself a source of the observed improvement, independent of the specific control law used.

4.5.2. Fixed reverse thrust produced large dispersion

The fixed reverse-thrust strategy improved stopping performance under some conditions; however, its effectiveness strongly depended on the selected thrust level. Since the reverse command remained constant regardless of vehicle speed or position, it could not adapt to variations in vehicle motion.

When the reverse thrust was insufficient, the braking force was unable to compensate for inertia, leading to overshoot. Conversely, excessive reverse thrust caused premature deceleration and unstable approach behavior. As a result, stopping performance became highly sensitive to operating conditions and exhibited significant run-to-run variability, as shown in Fig. 7 and Fig. 8.

The particularly large dispersion observed near f_r=125, confirmed by the follow-up sweep shown in Fig. 8(b), suggests a nonlinear or configuration-dependent response of the propulsion system. Possible mechanisms include motor efficiency changes, airflow interaction between the two fans, or other unmodeled dynamic effects; however, the present experiment does not contain sufficient diagnostic measurements to identify the dominant cause. Additional direct thrust measurements and propulsion-dynamics analysis would be required to distinguish these mechanisms.

4.5.3. Human operators appeared to utilize velocity information

When proportional reverse thrust was automatically superimposed on the single operator's manual forward control in Experiment 2, stopping performance became markedly less consistent than in Experiment 1, with large trajectory bulging and substantial run-to-run variation in the final position, as shown in Fig. 9. The operator was unable to reliably anticipate how the externallyimposedreverse thrust wouldinteract withthe operator's own input.

This result suggests that the single operator's stoppingbehaviorwas not basedsolelyonpositionerror;

however, the operator's decision-making process was not measured directly. The observation should therefore be interpreted as a finding from a single-operator experiment rather than evidence of a general human-control strategy. The result motivated the subsequent experiment using an explicit reference-speed profile.

4.5.4. Reference-velocity-based D control improved stopping performance

Based on the observations obtained from the single-operator experiment, a reference velocity profile was introduced and incorporated into the control system through velocity feedback. This approach enabled the controller to respond to deviations from the desired velocity profile rather than relying solely on position error. The contribution is not the derivative-control principle itself, which is well established, but its experimental application to the independently actuated double-fan configuration using a reference profile obtained from successful manual stopping runs.

Experimental results demonstrated that the proposed methodreducedthe average stopping-positionovershoot from approximately 9 mm to 3 mm (a reduction of roughly 67%) and significantly narrowed the trajectory dispersion compared with the conventional proportional control and the fixed reverse-thrust strategy (Fig. 10). These findings suggest that incorporating velocity information is effective for stopping control in systems characterized by significant inertia and actuation delay.

Because only a single operator was involved and the decision-making process was not directly measured, the experiment does not establish that human operators in general use velocity information in the same way. The reference-velocity controller was therefore evaluated as an independent control strategy rather than as a direct model of human decision-making.

4.5.5. Limitations of the present study

The experiments in this study were conducted using a single small-scale, ground-constrained platform under controlled laboratory conditions. Reynolds-number similarity and other dynamic-similarity conditions were not established, and theresultsare therefore not intended for quantitative extrapolation to a full-scale aircraft. In addition, thrust from the two fans was not measured independently, so the contributions of aerodynamic drag and active reverse thrust cannot be quantitatively separated from the present data. Because the vehicle was constrained to straight-line ground motion, pitching moment, angle of attack, and longitudinal flight stability were not measured. The control parameters were tuned specificallyforthe dynamics ofthisexperimental model, and external disturbances such as airflow interference and measurement noise were not explicitly varied. Finally, the manual experiment used a single operator, so the observations cannot be generalized to human operators in general. These limitations should be considered when interpreting the generalizability of the present results.

5. Conclusions and Future Work

Fundamental stopping-control experiments were conducted on a small ground-constrained model with independently commanded forward and reverse fans. The experiments showed that fixed reverse-thrust commands can change stopping accuracy and trajectory dispersion depending on the command level. A reference-velocity-based controller, derived from successful manual stopping trajectories and implemented using velocity feedback, reduced the average stopping-position overshoot from approximately 9 mm to 3 mm under the tested conditions and reduced trajectory dispersion. The principal contribution is therefore an experimental characterization of independently actuated forward/reverse fan control and the application of reference-velocity-based stopping control to this double-fan platform. The derivative-control principle itself is conventional, and the observed performance improvement should not be interpreted as a general result for all aircraft or propulsion systems.

Future directions include (i) direct thrust measurement to separate aerodynamic drag and active reverse-thrust effects, (ii) systematic controller tuning and uncertainty analysis, (iii) investigation of Reynolds-number and dynamic-similarity requirements before any full-scale extrapolation, (iv) measurement of additional vehicle and propulsion states relevant to pitch and stability, (v) evaluation with multiple operators if human-control generalization is required, and (vi) comparison with alternative braking configurations such as single-propeller or throttle-reduction strategies..

Acknowledgments

The authors thank the members of the Toda Laboratory for their helpful discussions and technical support. This work was conducted as part of an undergraduate research project at the University of Toyama.

References

[1] T. I. Fossen, Handbook of Marine Craft Hydrodynamics and Motion Control. Chichester, U.K.: John Wiley & Sons, Apr. 2011. https://doi.org/10.1002/9781119994138

[2] M. Kondo, Aircraft Motion and Control. Tokyo, Japan: Sangyo Tosho, 1985. [In Japanese].

[3] Ministry of Land, Infrastructure, Transport and Tourism (MLIT), Roadmap toward practical use of autonomous merchant ships, Aug. 2018. [In Japanese]. https://www.mlit.go.jp/common/001237409.pdf

[4] International Maritime Organization (IMO), Interim guidelines for MASS trials, MSC.1/Circ. 1604, 2019.

[5] V. Bertram, Autonomous ships, in Proceedings of the 15th International Conference on Computer Applications and Information Technology in the Maritime Industries. (COMPIT), 2016, pp. 10–21.

[6] K. Hasegawa, Trends and future outlook for maritime autonomous surface ships (MASS), KANRIN, vol. 83, pp. 1–8, 2019. [In Japanese].

[7] K. Terashima, Present status and future prospects of autonomous ship technology, Koukai (J. Japan Inst. Navig.), no. 200, pp. 45–52, 2017. [In Japanese].

[8] K. Shoji, Ship Operation and Safety. Tokyo, Japan: Seizando Shoten, 2014. [In Japanese].

[9] Japan Transport Safety Board, Analysis report on marine accidents: Toward prevention of human-factor accidents, 2021. [In Japanese].

[10] Marine Accident Tribunal of Japan, Marine casualty statistics by type and cause (Reiwa 4), 2023. [In Japanese].

[11] A. M. Rothblum, Human error and marine safety, National Safety Council Congress and Exposition, vol. 2, pp. 1–12, 2000.

[12] A. Otani et al., Analysis of mental models and decision criteria of expert ship operators, J. Japan Inst. Navig., vol. 115, pp. 211–218, 2006. [In Japanese].

[13] J. Fukuto, Research on automatic berthing control of ships, Natl. Maritime Res. Inst. Rep., vol. 30, no. 5, pp. 245–312, 1993. [In Japanese].

[14] K. Hasegawa, Current status and issues in automating berthing and unberthing maneuvers, Koukai, no. 180, pp. 32–38, 2012. [In Japanese].

[15] T. Yamazu et al., Construction of an automatic berthing control system using tugboats, Proc. Japan Soc. Naval Architects Ocean Eng., no. 26, pp. 373–376, 2018. [In Japanese].

[16] H. Sato et al., Fundamental experiments on station-keeping control of a small model using camera feedback, Trans. Soc. Instrum. Control Eng., vol. 52, no. 4, pp. 220–227, 2016. [In Japanese].

[17] Y. Ogawa et al., Maneuvering characteristics and control of ships in the low-speed regime, J. Japan Soc. Naval Architects Ocean Eng., no. 25, pp. 105–115, 2017. [In Japanese].

[18] S. Motoda, Environmental disturbances and nonlinear ship motions during berthing and unberthing, in Proc. 27th Ship Mechanics Symp., 2015. [In Japanese].

[19] S. Kuwahara et al., Development of target detection and automatic collision-avoidance algorithms for ships using deep learning, J. Japan Inst. Navig., vol. 141, pp. 165–173, 2019. [In Japanese].

[20] N. Suda, PID Control. Tokyo, Japan: Asakura Publishing, 1992. [In Japanese].

[21] J. J. Hart and J. L. Devolites, NASA Johnson Space Center, Morpheus: Advancing technologies for human exploration, in Proc. AIAA SPACE 2014 Conf. Expo., San Diego, CA, USA, Aug. 2014, https://doi: 10.2514/6.2014-4441

[22] J. J. Hart and J. L. Devolites, The tailoring of traditional systems engineering for the Morpheus project, in Proc. AIAA SPACE 2013 Conf. Expo., San Diego, CA, USA, 2013.

[23] H. Glauert, Airplane propellers, in Aerodynamic Theory, vol. IV, W. F. Durand, Ed. Berlin, Germany: Springer-Verlag, 1935, pp. 169–360.

[24] B. W. McCormick, Aerodynamics, Aeronautics, and Flight Mechanics, 2nd ed. New York, NY, USA: Wiley, Sep. 1994.

[25] H. Nouri, F. Ravelet, F. Bakir, C. Sarrat, and R. Rey, Design and experimental validation of a ducted counter-rotating axial-flow fans system, Journal of Fluids Engineering, vol. 134, iss. 10, Oct. 2012, Art. no. 104504. https://doi.org/10.1115/1.4007591